DGFI Report
No. 83

Separation of oceanic and hydrological mass variations by simulated gravity observations

Martin Schmeer, Wolfgang Bosch, Michael Schmidt

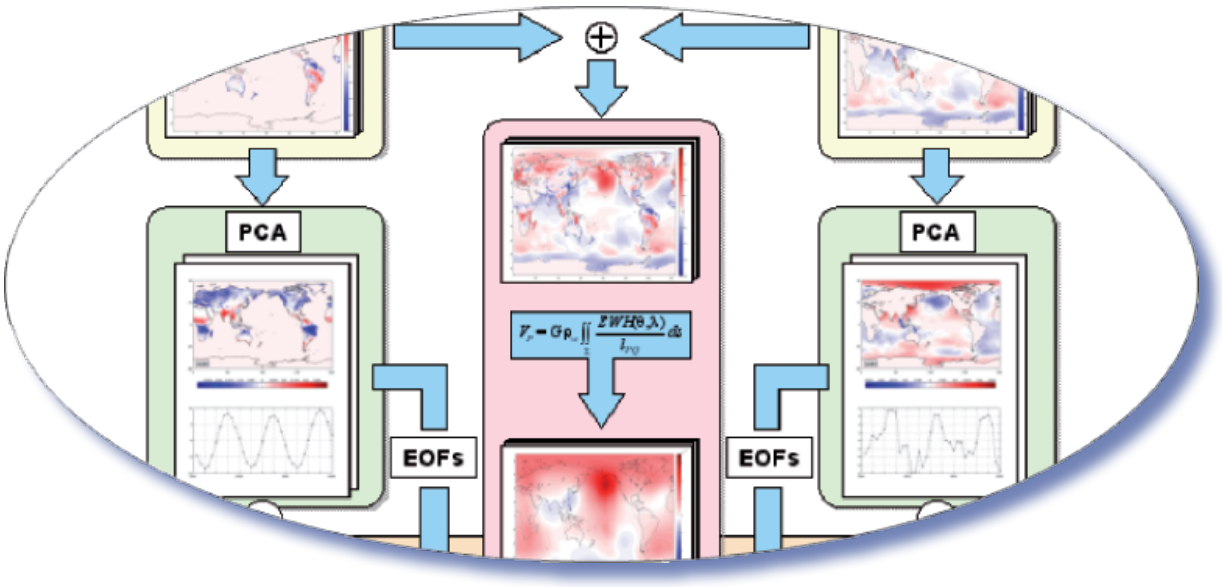

Deutsches Geodätisches Forschungsinstitut
Alfons–Goppel–Str. 11, D–80539 München, Germany
2008

Deutsches Geodätisches Forschungsinstitut
Alfons–Goppel–Str. 11
D – 80539 München

Tel.: +49 89 23031–1119
Fax: +49 89 23031–1240

email: mailer@dgfi.badw.de

htpp://www.dgfi.badw.de

Table of Content

Abstract

Mass variations within the Earth's subsystems atmosphere, oceans and continental hydrosphere are comprised in geodetic measurements and can be monitored by observations of the satellite gravity mission GRACE. The observations yield integral signals and cannot distinguish between different processes or components. It is a challenging problem to separate the spatio-temporal signals from the different subsystems each characterized by an individual spectral behaviour. In this contribution a spatial separation is discussed by applying principal component analysis (PCA) to specific geophysical models for the non-overlapping regions oceans and continents. The set of all empirical orthogonal base functions (EOFs) from both PCAs establishes the vector space for a joint estimation of the unknown parameters of the functional model. To check this procedure gravity field observations from given geophysical models are simulated in order to try recovering the time-dependent coefficients, i.e., the principal components (PCs) from parameter estimation. The estimated PCs show excellent correlations (larger than 0.9) comparing the original PCs even with a limited number of EOFs.

1 Introduction

Mass variations and mass displacements within atmosphere, oceans and continental hydrosphere cause time-dependent variations in the Earth's gravity field. Gravity field observations such as the K-band range (KBR) measurements of the satellite gravity field mission GRACE (Gravity Recovery and Climate Experiment), however, monitor the integral gravitational effect [TAPLEY ET AL., 2004]. Whereas the temporal variability of mass distributions is determined from gravity changes which are observed by this satellite gravity mission and from height changes of water and ice surfaces which are simultaneously observed by satellite altimetry missions. At present the processing of GRACE data requires the removal of short term mass variations in the subsystems atmosphere and the oceans in a so-called de-aliasing procedure. More precisely, the time varying forces caused by these subsystems have to be eliminated prior to or during the gravity field determination using external data sources [FLECHTNER, 2005]. A successful identification and separation of individual mass signals transmitted from the Earth's subsystems means still the most challenging problem within the data processing of the satellite gravity mission GRACE. Therefore, the fundamental question

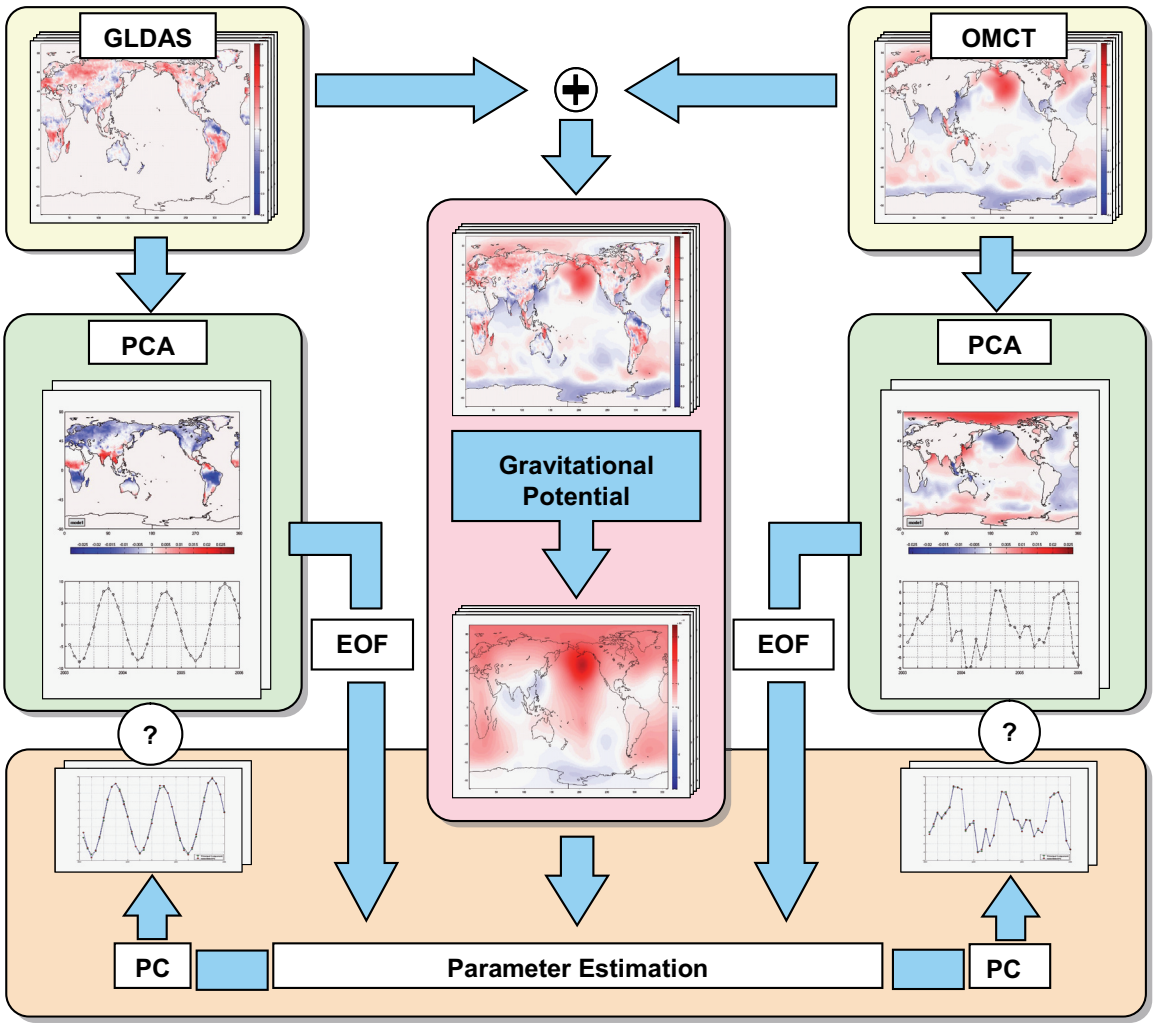

Figure 1: Flowchart for the separation of individual effects from simulated integral gravity potential data. The separation is performed by mass signals of geophysical models for the subsystems oceans and continental hydrology.

arises if it is possible at all to identify and separate mass variations within the aforementioned compartments from the integral GRACE observations. In this contribution the joint gravity effect of the oceans and the continental hydrosphere is investigated by applying principal component analysis (PCA) to geophysical models for the non-overlapping regions land and ocean in a pre-processing step. Figure 1 gives an overview of the implemented scheme utilising the orthogonality of the base functions related to land and oceans, respectively. It appears that a spatial separation is possible proven by a closed-loop simulation

2 Model data sets and their processing

Mass variations and redistributions within the subsystems oceans and continental hydrosphere are comprised in several geophysical models. In this report data sets from the numerical models OMCT (Ocean Model for Circulation and Tides) for the oceans [THOMAS 2002] and GLDAS (Global Land Data Assimilation System) for the continental hydrology [RODELL ET AL. 2004] have been used. Details of both models are listed below in the tables 1 and 2.

Table 1: Overview of basic model parameters of the hydrological model GLDAS

Forcing	Multiple data sets derived from satellite measurements and atmospheric analyses
Coverage	All continental regions north to 60 degrees S
Spatial resolution	1.0° × 1.0°
Output	– equivalent water height – snow cover – soil moisture – surface temperature – leaf area index

Table 2: Overview of basic model parameters of the ocean model OMCT

Forcing	Wind stress/velocity, heat flux, atmospheric pressure from ECMWF analyses, freshwater fluxes from ECMWF forecasts
Coverage	Global, 77°S – 90°N
Spatial resolution	1.875° × 1.875°, 13 levels
Output	– oceanic bottom pressure (contribution of the water column alone) – atmospheric pressure at sea level – sea level height

The parameter ocean bottom pressure from OMCT has to be converted into a mass equivalent water height (EWH) according to

$$EWH = \frac{bp}{\rho_{SW} \; g_0} \tag{1}$$

The bottom pressure is denoted as *bp*, the density of saltwater as ρ_{sw} (1025 kg/m³) and the mean gravitational acceleration as g_0, respectively. The quan-

tity EWH has to be interpreted as a load: an EWH of 1 m corresponds to a pressure of 98 hPa in case of $\rho_w = 1000 kg/m^3$. Next the EWHs of OMCT are transformed to a 1° grid comparable to the spatial resolution of the hydrology model GLDAS. Data sets of both models are available as monthly mean fields for 36 time steps from January 2003 to December 2005. Moreover mass variations are calculated as variations relative to the mean of these three years. Figure 2 represents mass variations for one single time step of hydrology, oceans and the sum of both. To avoid a consideration of masses in coastal areas twice due to an improper conformity of both models, a land ocean mask is used due to the data set of GLDAS.

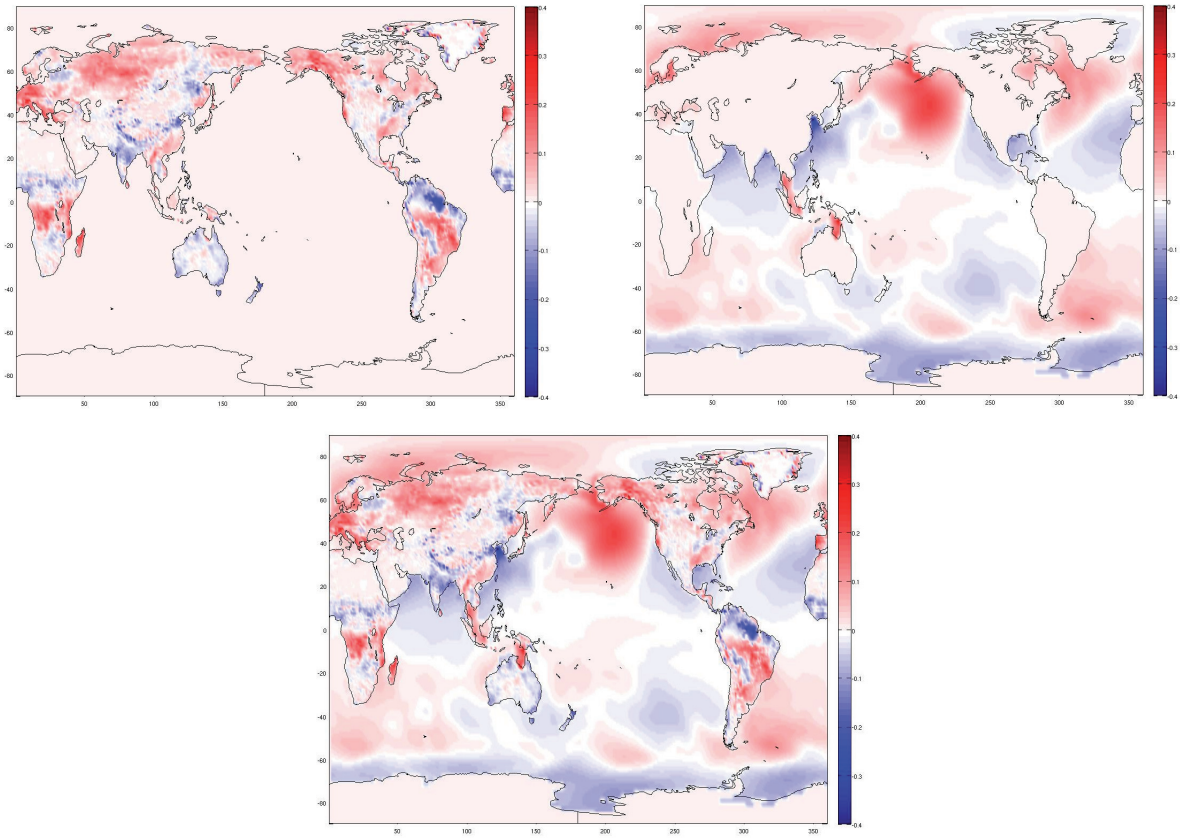

Figure 2: EWHs [m] from the hydrology model GLDAS (top left) and from the ocean model OMCT (top right) and the sum of both models (bottom) for January 2003

3 Principal Component Analysis (PCA)

Applying principal component analysis (PCA) a spatio-temporal input signal, e.g., a data set from the ocean model OMCT can be expanded into a series in terms of orthonormal spatial base functions denoted as empirical orthogonal functions (EOFs). The corresponding series coefficients, i.e. the principal components (PCs), represent the temporal behaviour of the input signal. The EOFs are derived from an eigenvector and eigenvalue decomposition of the empirical covariance matrix of the input signal; the PCs are the result of the transformation of the signal into the space spanned by the EOFs. In other words PCA identifies the geographical patterns (EOFs) together with their temporal evolution (PCs). Since the EOFs are related to the eigenvalues the

input signal can be separated into dominant and non-dominant parts (modes) [PREISENDORFER 1988]. In our investigation we identify the input signal with an EWH data set and define

$$EWH(\theta,\lambda,t) = \sum_{i=1}^{I_{\max}} EOF_i(\theta,\lambda)\, c_i(t) \tag{2}$$

Herein θ and λ are geographical latitude and longitude, respectively, t means the time and $i = 1, \ldots, I_{max}$ is the counting index for the modes. Note, the first mode (i=1) comprises the most dominant structures of the EWHs. For each of the two subsystems, i.e. oceans and continental hydrosphere, an independent PCA was applied to the EWHs given within the chosen observation interval (cf. Appendix). As can be seen from Fig. 3 for OMCT about 90% of the total variance of the mass variations is described by $I_{max} = 14 =: I$ modes; for GLDAS 90% are exceeded by $I_{max} = 7 =: J$ modes. Since the two compartments, oceans and continents are non-overlapping the set of base functions, i.e. the EOFs related to the 21 dominant eigenvalues, establish an orthogonal basis of a subspace of the parameter space. The corresponding PCs are the unknown parameters of the adjustment problem discussed in section 5.

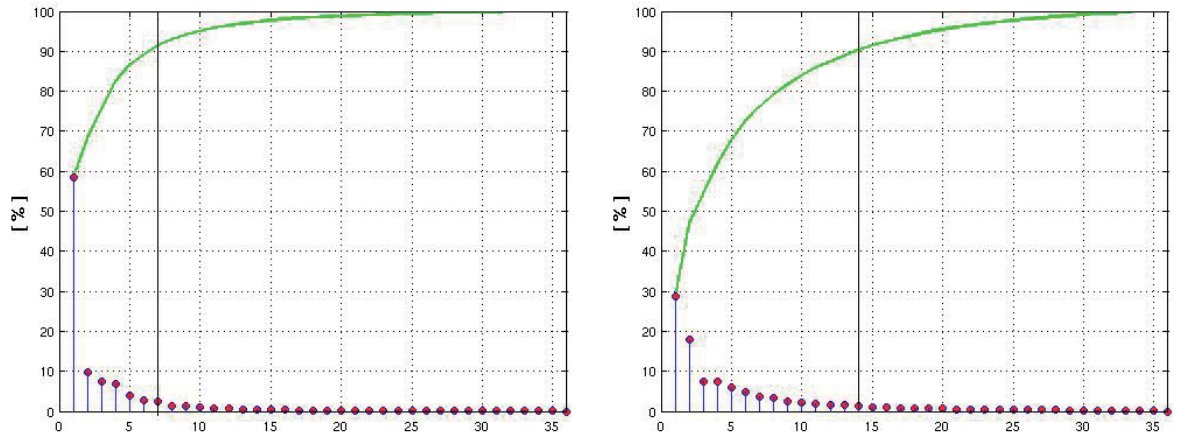

Figure 3: Percentages of the eigenvalues to the total variance for hydrology (left) and ocean (right). The green lines above the bars mark the accumulated portion of the eigenvalues, the black upright lines visualize the limit of 90% of the total variance; consequently 7 modes for hydrology and 14 modes for the oceans are necessary.

4 Simulating Gravitational Potential

In order to check our method we simulate gravity field observations from GRACE. The gravitational potential V_P is computed from the combination of the two geophysical models OMCT and GLDAS. Their single EWH contributions are added together to one mass equivalent layer for each time step according to the Newton's Integral

$$V_P = G \iiint_{\Sigma} \frac{dm}{l_{PQ}} = G\,\rho_w \iint_{\Sigma} \frac{EWH(\theta,\ \lambda)}{l_{PQ}}\, ds \tag{3}$$

HEISKANEN AND MORITZ [1985]. Herein G and ρ_w denote the gravitational constant and the density of water, respectively.

l_{PQ} stands for the distance between the attracted point $P(\theta_P, \lambda_P, r_P)$ and the surface element ds located at $Q(\theta, \lambda, R)$

$$l_{PQ} = \sqrt{r_P^2 + R^2 - 2Rr_P \cos\psi}$$

$$\cos\psi = \cos\theta_P \cos\theta_Q + \sin\theta_P \sin\theta_Q \cos(\lambda_Q - \lambda_P)$$

Here we calculated the gravitational potential at the spherical surface Σ of the Earth , i.e. for $r_P = R$ and for the GRACE orbital height of around $r_P = R + 500\ km$. In order to deal with more realistic GRACE input data we added white noise with a standard deviation of $\sigma = 0.003 m^2/s^2$. Figure 4 shows the simulated gravitational potential input data at GRACE orbital height for a specific time. A feasible spatial reduction to a 1.8° grid is done since GRACE monthly gravitational fields are developed up to spherical harmonic degree and order 100.

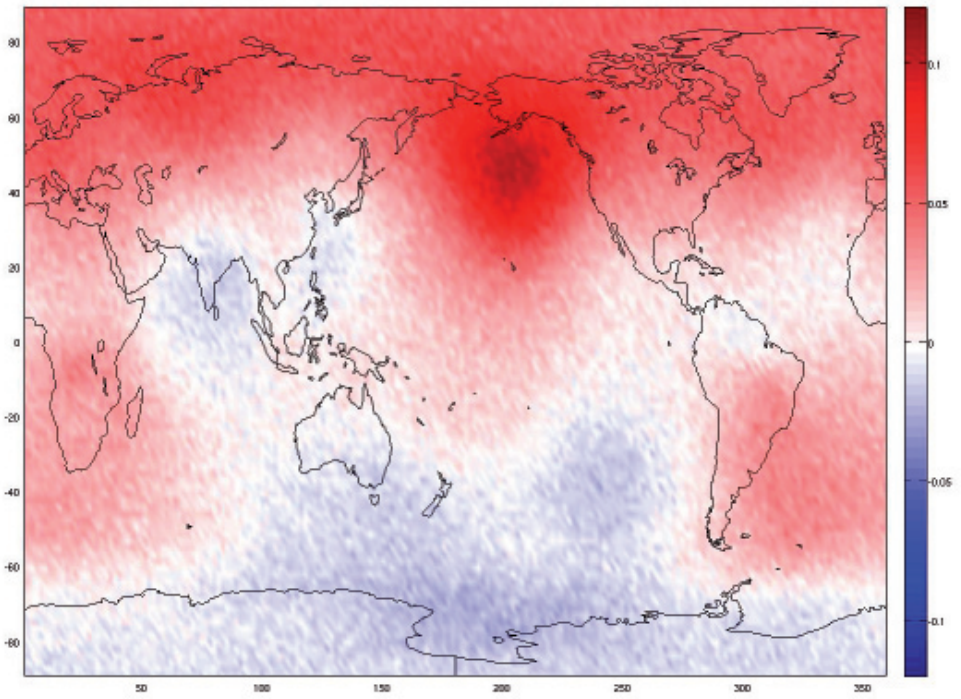

Figure 4: Simulated gravitational potential [m²/s³] from GLDAS over land and OMCT over oceans at time January 2003 including white noise (standard deviation σ = 0.003m²/s²) at GRACE orbital height.

5 Parameter Estimation

Next we introduce Equation (2) into the right-hand side of Equation (3) and obtain the observation equation

$$\begin{aligned} V(\theta_P,\lambda_P,t) &= G\rho_w \iint_\Sigma \frac{1}{l_{PQ}} \left(\sum_{i=1}^{I} EOF_{i,o}(\theta,\lambda) c_{i,o}(t) + \sum_{j=1}^{J} EOF_{j,h}(\theta,\lambda) c_{j,h}(t) \right) ds \\ V(\theta_P,\lambda_P,t) &= G\rho_w \sum_{i=1}^{I} c_{i,o}(t) \underbrace{\iint_\Sigma \frac{1}{l_{PQ}} EOF_{i,o}(\theta,\ \lambda)\, ds}_{a_{i,o}(\theta_P,\lambda_P)} + G\rho_w \sum_{j=1}^{J} c_{j,h}(t) \underbrace{\iint_\Sigma \frac{1}{l_{PQ}} EOF_{j,h}(\theta,\lambda)\, ds}_{a_{j,h}(\theta_P,\lambda_P)} \end{aligned} \quad (4)$$

for the simulated spatio-temporal GRACE input signal $V(t)$. In this equation the coefficient sets $c_{i,o}$ and $c_{j,h}$ are the unknown parameters of the ocean and the hydrology model parts, respectively. Since the simulated input signal is given globally at 36 discrete times $t = t_k$ for $k = 1, \ldots, K = 36$ we solve for altogether $u = 21 \times 36 = 756$ unknowns with $u_1 = 21$ and $u_2 = 36$. On the right-hand side of the observation equation (4) a transformation of the EOFs into *integro-base-functions* $a_{i,o}(\theta_P,\lambda_P)$ and $a_{j,h}(\theta_P,\lambda_P)$ has been performed.

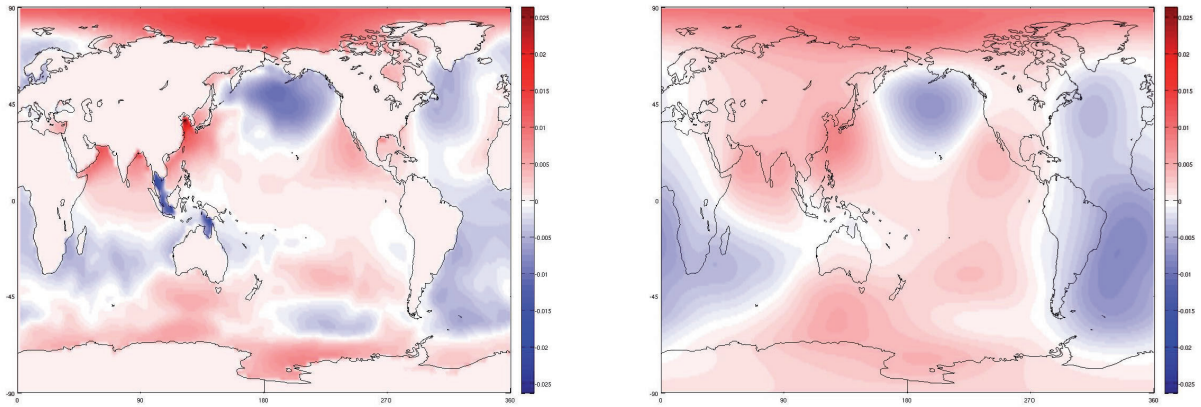

Figure 5: Empirical orthogonal function (EOF) for mode 1 of the ocean model OMCT (left) and its integro-base-function a_1 for GRACE orbit height r_p = R+500 km (right)

Whereas, as mentioned before, the EOFs establish an orthogonal basis of the parameter sub space, the transformed base functions $a_{i,o}(\theta_P,\lambda_P)$ and $a_{j,h}(\theta_P,\lambda_P)$, however, do not fulfil this favourable property because of the integration (see example shown in Fig.5). Collecting all N gravitational potential observations $V(t_k) = V(\theta_P,\lambda_P,t_k)$ with $P = 1, \ldots, N$ into an $N \times 1$ observation vector $\boldsymbol{y}_k$, defining the $u \times 1$ vector

$$\mathbf{c}_k = \left[c_{1,h}(t_k) \quad \ldots \quad c_{1,o}(t_k) \quad \ldots\right]' = \left[\mathbf{c}_{h,k} \quad \mathbf{c}_{o,k}\right]'$$

wherein $\mathbf{c}_{h,k}$ and $\mathbf{c}_{o,k}$ are $u_1 \times 1$ and $u_2 \times 1$ vectors of the unknown series coefficients $c_{i,h}(t_k)$ and $c_{j,o}(t_k)$. Furthermore, we define the $N \times$ u matrix

$$\mathbf{A} = \begin{bmatrix} a_{1,h}(\theta,\lambda)_1 & \cdots & a_{1,o}(\theta,\lambda)_1 & \cdots \\ a_{1,h}(\theta,\lambda)_2 & \cdots & a_{1,o}(\theta,\lambda)_2 & \cdots \\ \cdots & \cdots & \cdots & \cdots \\ a_{1,h}(\theta,\lambda)_N & \cdots & a_{1,o}(\theta,\lambda)_N & \cdots \end{bmatrix} = \left[\mathbf{A}_h \quad \mathbf{A}_o\right]$$

wherein $\mathbf{A}_h$ is an $N \times u_1$ and $\mathbf{A}_o$ is an $N \times u_2$ matrix. Next we define the $N \times K$ observation matrix

$$\mathbf{Y} = \left[\mathbf{y}_1 \quad \ldots \quad \mathbf{y}_K\right]'$$

and the $u \times K$ matrix

$$\mathbf{C} = \left[\mathbf{c}_1 \quad \ldots \quad \mathbf{c}_K\right]'$$

of the unknown parameters. Assuming equal weights for each set of gravitational potential data we formulate the multivariate Gauss-Markov model

$$\mathbf{AC} = E(\mathbf{Y}) \quad with \quad D(vec\ \mathbf{Y}) = \boldsymbol{\Sigma} \otimes \mathbf{I} \tag{5}$$

(Koch 1999); $E(...)$ and $D(...)$ mean the expectation vector and the covariance matrix, respectively, *vec* is an operator which orders the columns of a matrix

one below the other as a vector; $\mathbf{I}$ is the $N \times N$ unit matrix, $\mathbf{\Sigma}$ a $K \times K$ unknown covariance matrix. The least squares adjustment yields the estimation

$$\hat{\mathbf{C}} = (\mathbf{A}'\mathbf{A})^{-1}\mathbf{A}'\mathbf{Y} \tag{6}$$

of the unknown parameter matrix. The corresponding covariance matrix reads

$$D\left(vec\hat{\mathbf{C}}\right) = \Sigma \otimes (\mathbf{A}'\mathbf{A})^{-1} \tag{7}$$

6 Results and Discussion

Figure 6 shows the correlation matrix of the estimated matrix of the unknown parameters. As discussed before the correlation matrix is not diagonal anymore but diagonal dominant, i.e. the correlations between the estimated series coefficients are mainly small, especially between the ocean and the hydrology model parts (smaller than 0.1). This fact shows that separation between the effects of the subsystems oceans and hydrology is possible, even for a limited number of EOF base functions.

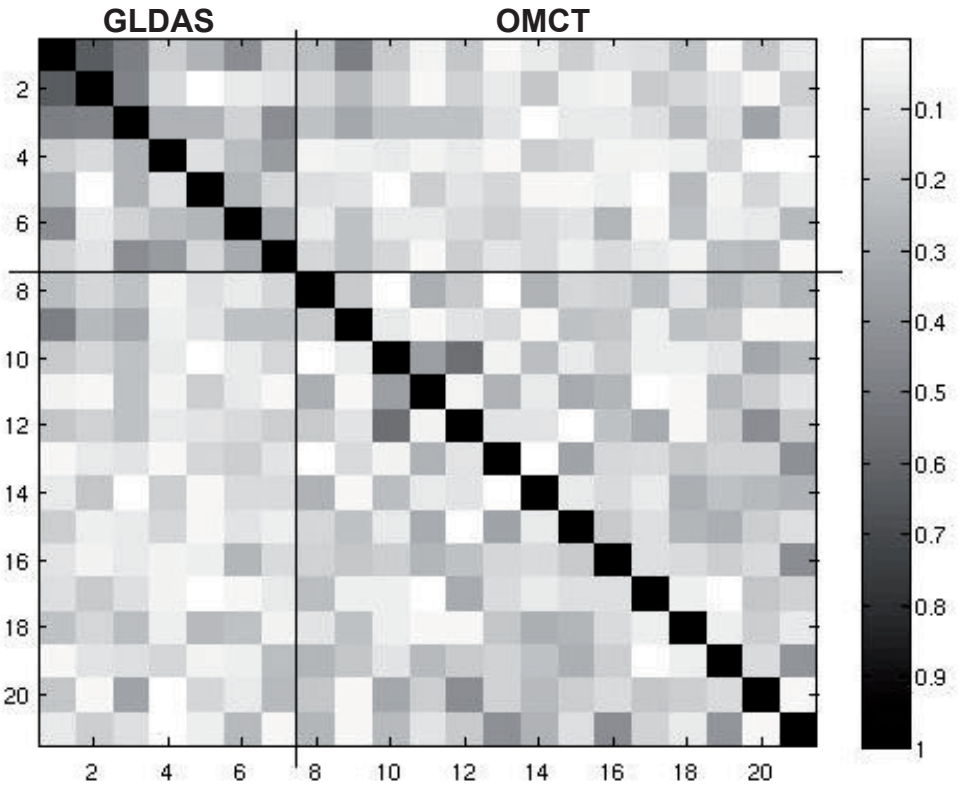

Figure 6: Correlation matrix of the estimated series coefficients introduced in Equation (4) for one single time step. The first seven rows and columns are related to the hydrology model part, the submatrix bottom right shows the correlation behaviour of the oceanic model part. It can be seen that between the model parts the correlations are very small or even negligible.

Only the first three coefficients of the hydrology model part are characterized by correlation values up to 0.7. These higher correlations could be explainable by a significant seasonal signal dominating the principal components

from mode 1 to 3 of the hydrological model (see Fig. A9, A11, A13).
The performed simulation proves that oceanic and hydrological mass variations can be spatially separated. We show that it is feasible demerging an integral signal into its partial signals. However bearing in mind this approach is only a consideration under nearly ideal conditions. Outlooking future work will consider atmospheric effects as well as the application of real GRACE data time series. Concurrently this simulation will be done soon for other oceanic and hydrological models and combinations of them.

References

Flechtner, F.: AOD1B Product Description Document, GRACE Proj. Doc. JPL 327-750, rev. 2.1, Jet Propul. Lab., Pasadena, Calif., 2005.

Koch, K.R.: Parameter estimation and hypothesis testing in linear models. Springer, Berlin, 1999

Preisendorfer, R. W.: Principal component analysis in Meteorology and Oceanography. New York: Elsevier, 1988.

Rodell, M., P. R. Houser, U. Jambor, J. Gottschalck, K. Mitchell, C.-J. Meng, K. Arsenault, B. Cosgrove, J. Radakovich, M. Bosilovich, J. K. Entin, J. P. Walker, D. Lohmann, and D. Toll: The Global Land Data Assimilation System. Bull. Amer. Meteor. Soc., 85 (3), 381394, 2004.

Tapley, B., S. Bettadpur, M. Watkins, and C. Reigber: The gravity recovery and climate experiment: mission overview and early results. Geophy. Res. Lett., 31(9), L09607,doi:10.1029/2004GL019920, 2004.

Thomas, M.: Ozeanisch induzierte Erdrotationsschwankungen - Ergebnisse eines Simultanmodells für Zirkulation und Gezeiten im Weltozean. PhD thesis, University Hamburg, 2001.

Appendix

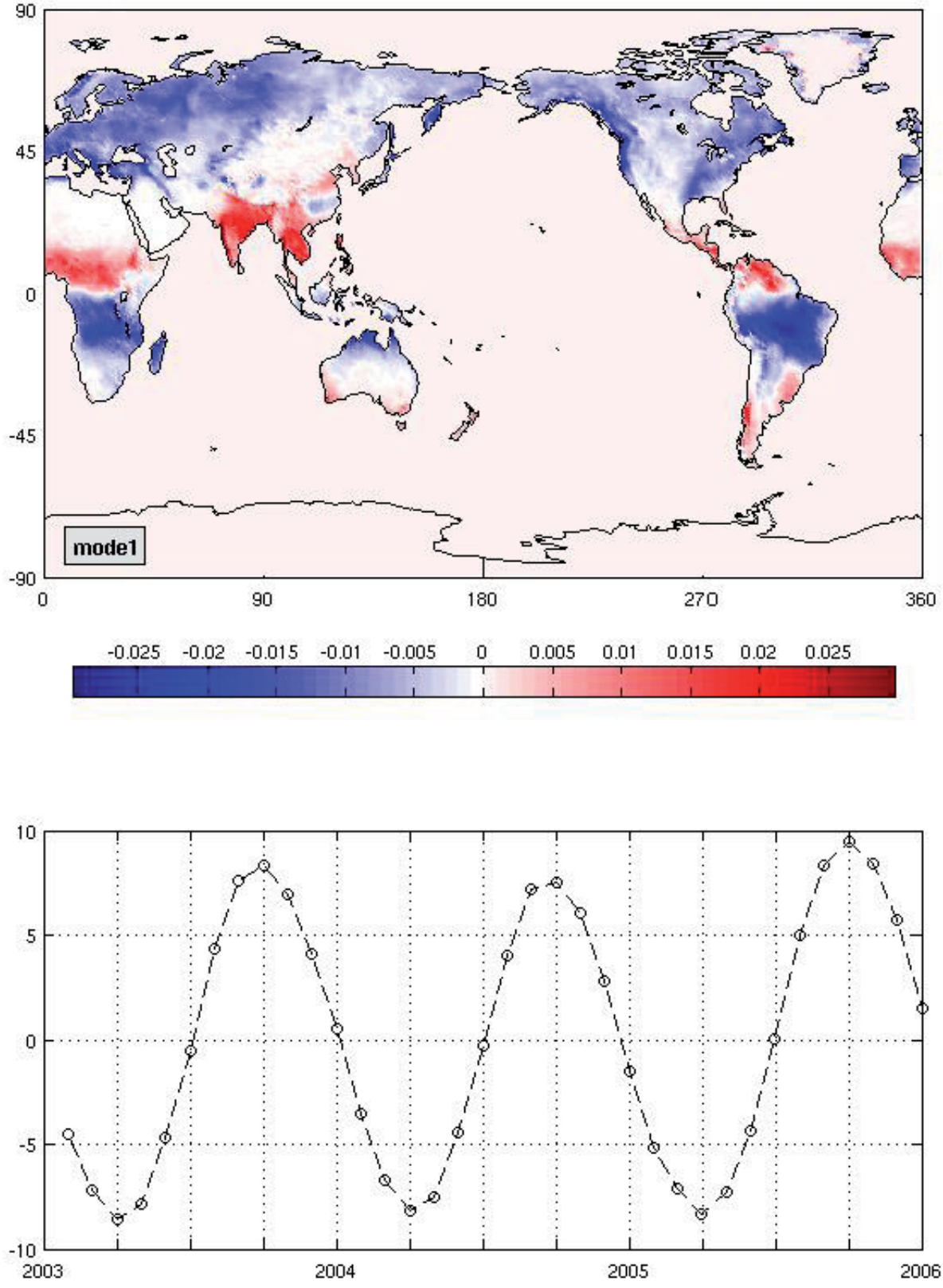

A1: Eigenvector (upper panel) and principal components (lower panel) of mode 1 for the compartment continental hydrology

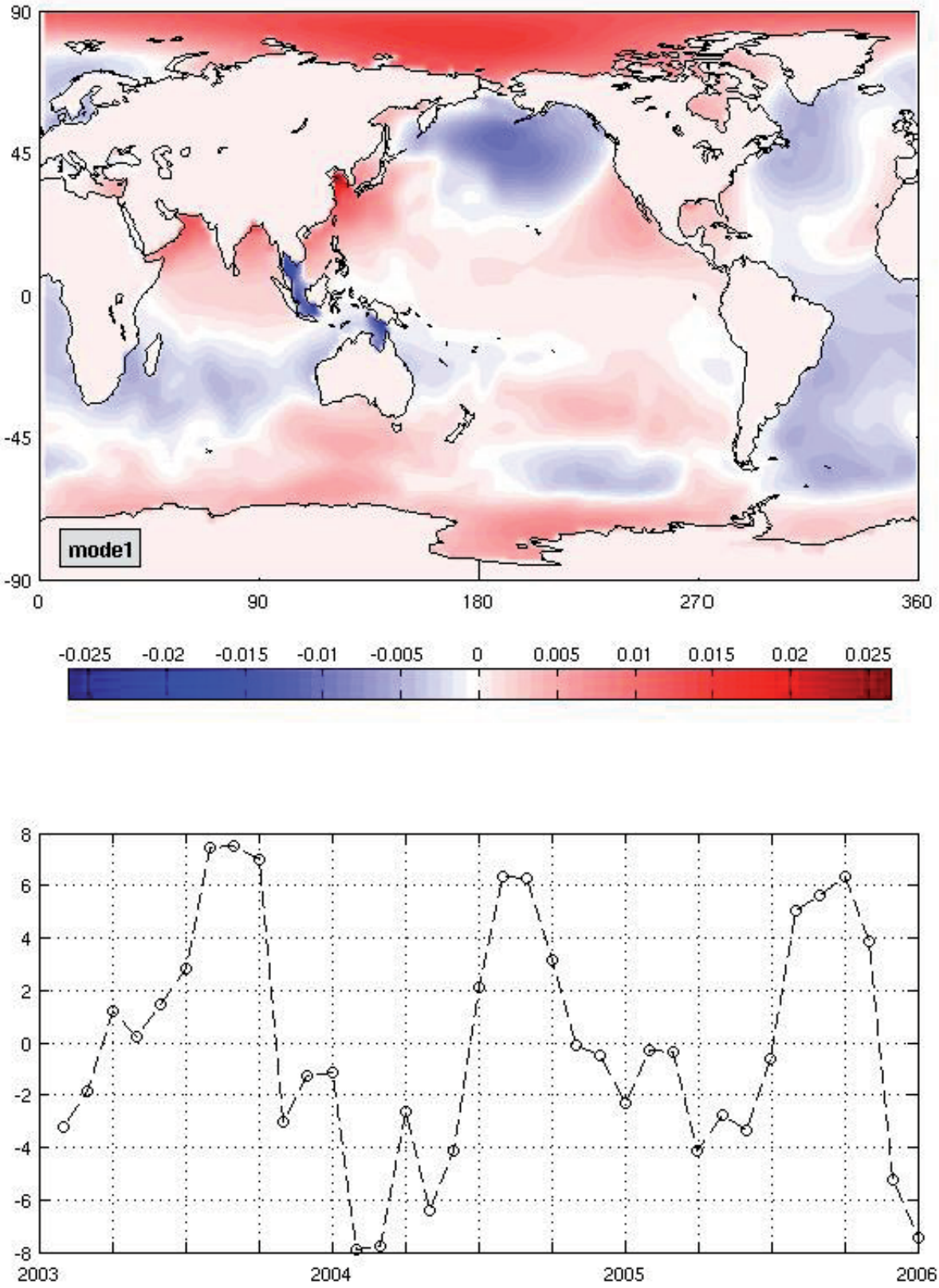

A2: Eigenvector (upper panel) and principal components (lower panel) of mode 1 for the compartment ocean

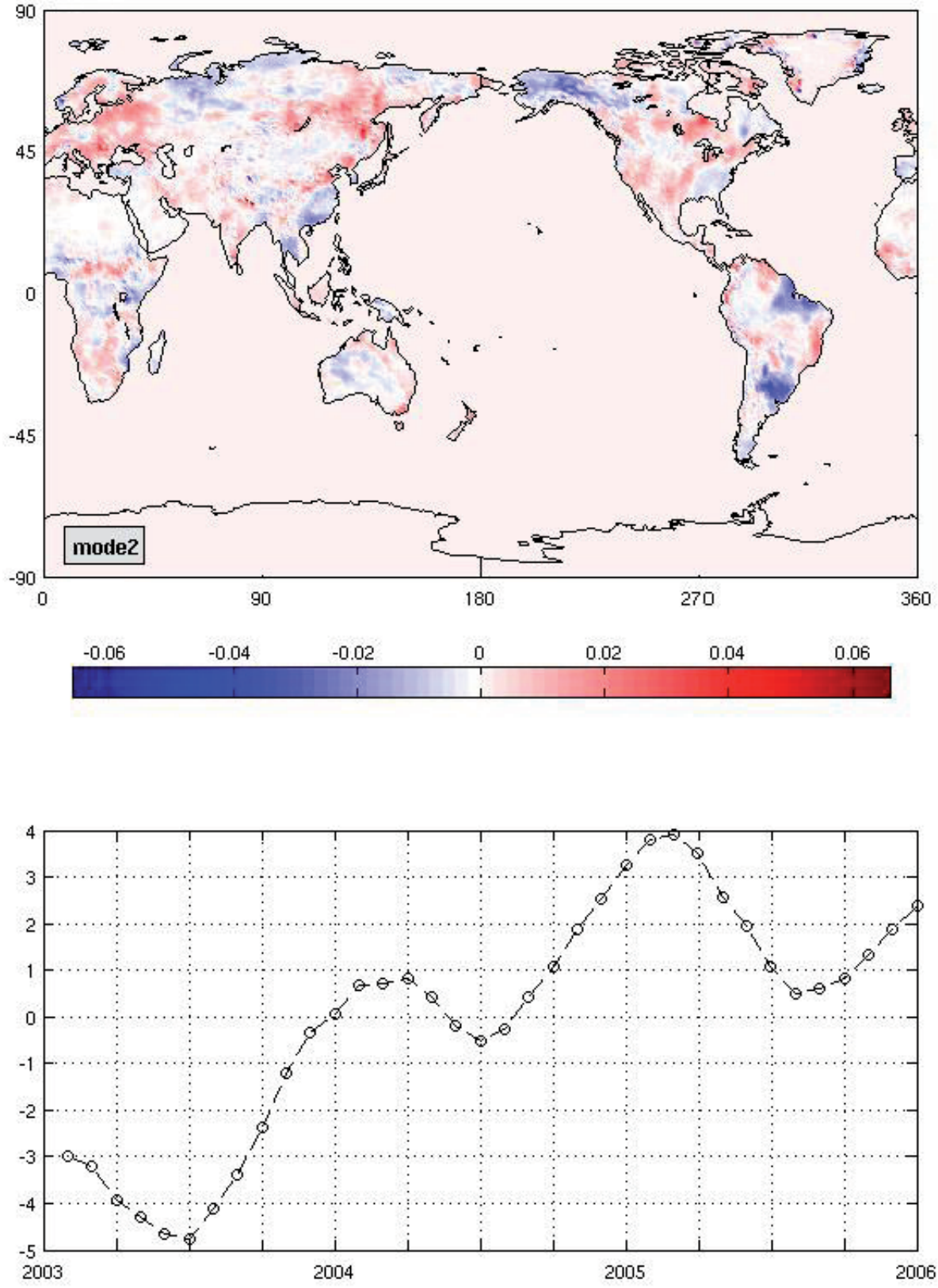

A3: Eigenvector (upper panel) and principal components (lower panel) of mode 2 for the compartment continental hydrology

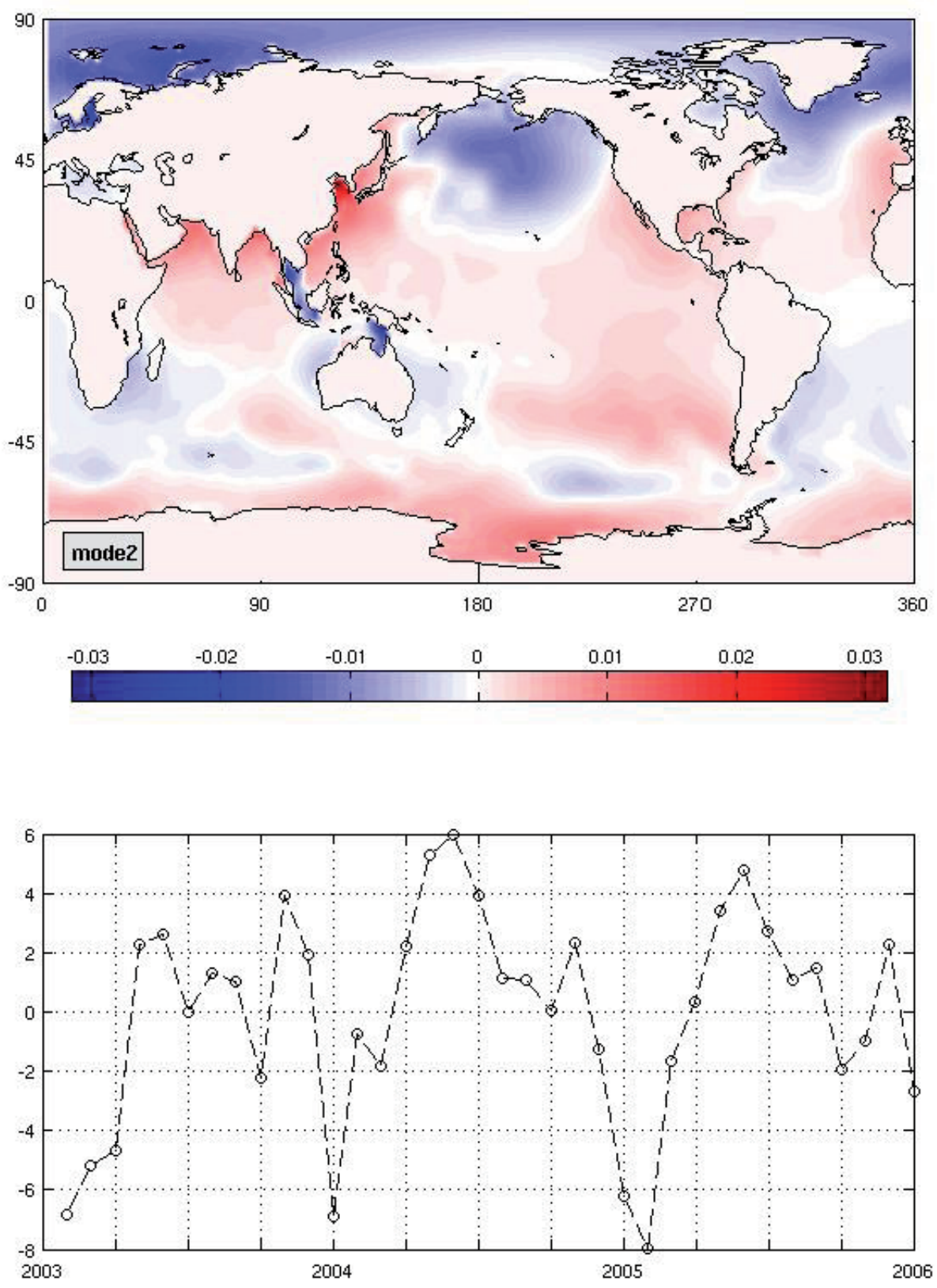

A4: Eigenvector (upper panel) and principal components (lower panel) of mode 2 for the compartment ocean

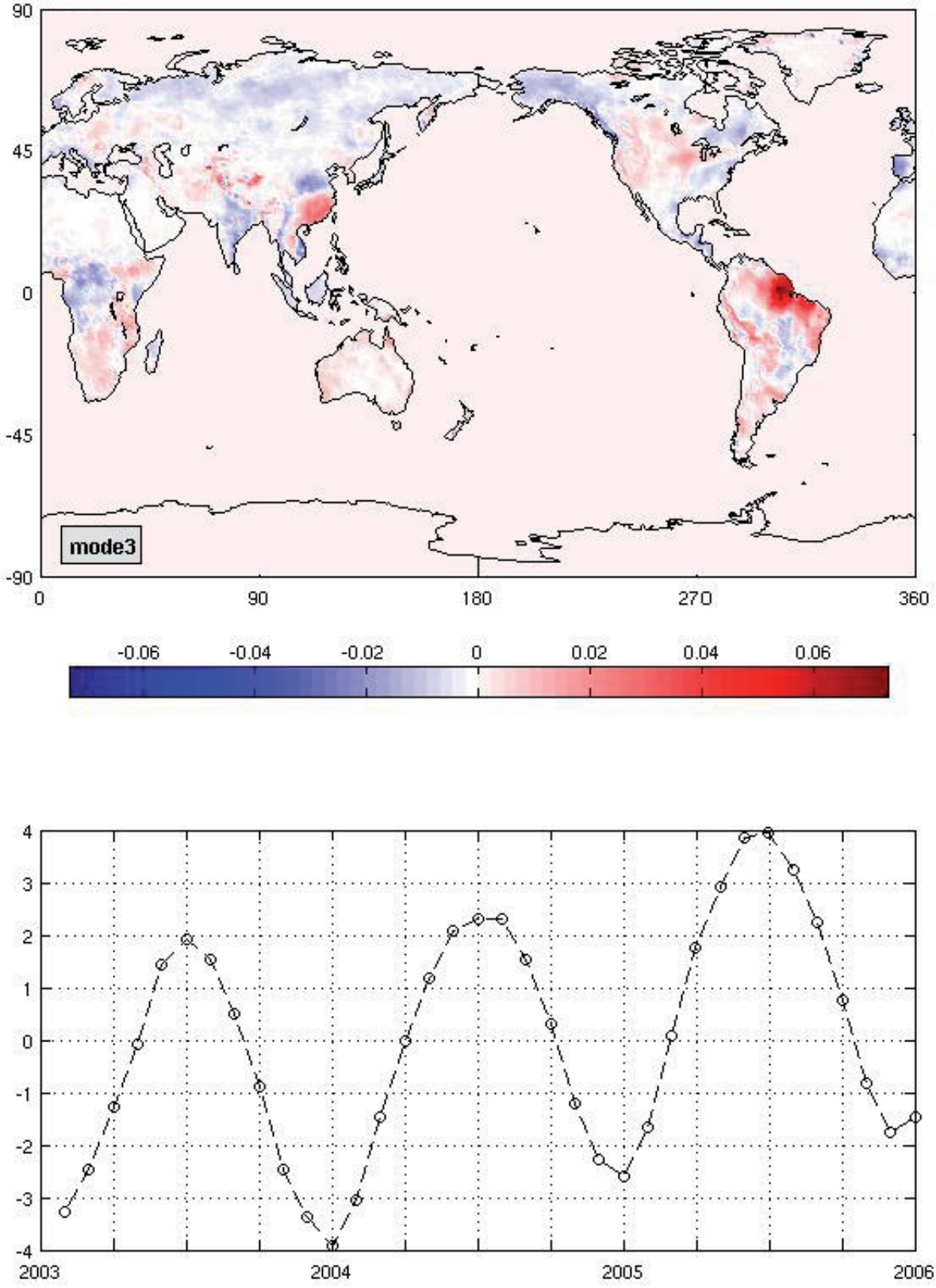

A5: Eigenvector (upper panel) and principal components (lower panel) of mode 3 for the compartment continental hydrology

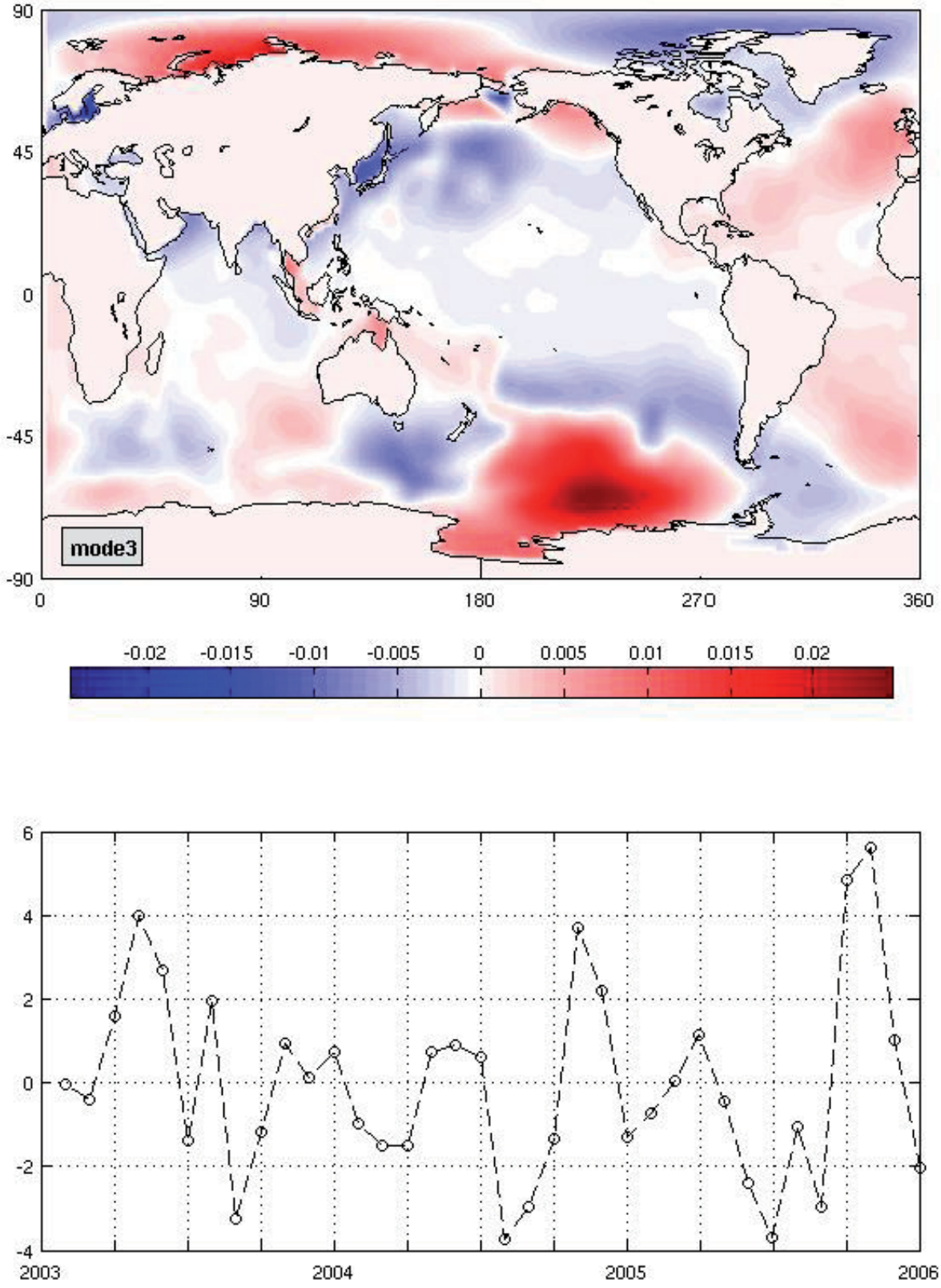

A6: Eigenvector (upper panel) and principal components (lower panel) of mode 3 for the compartment ocean

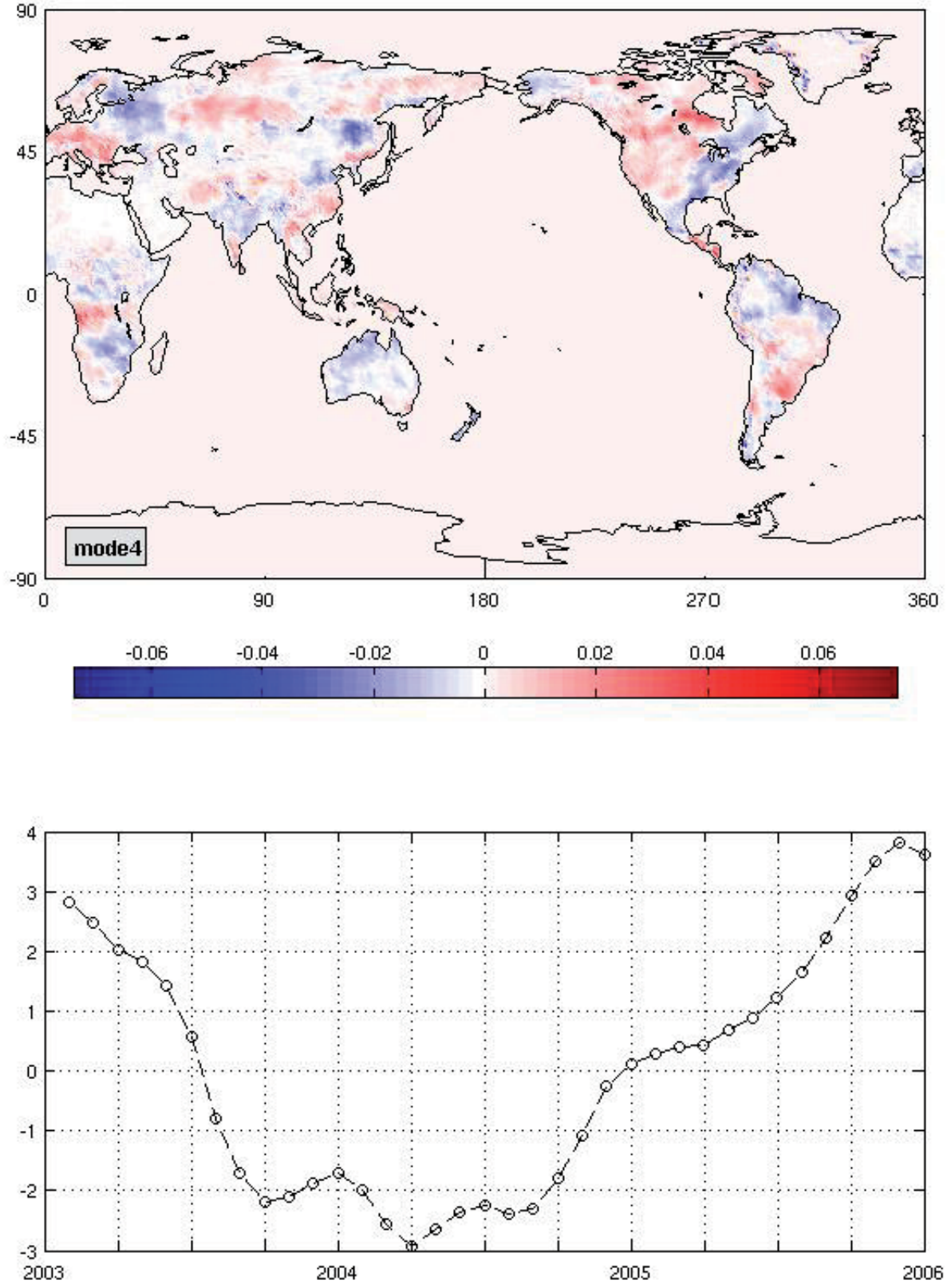

A7: Eigenvector (upper panel) and principal components (lower panel) of mode 4 for the compartment continental hydrology

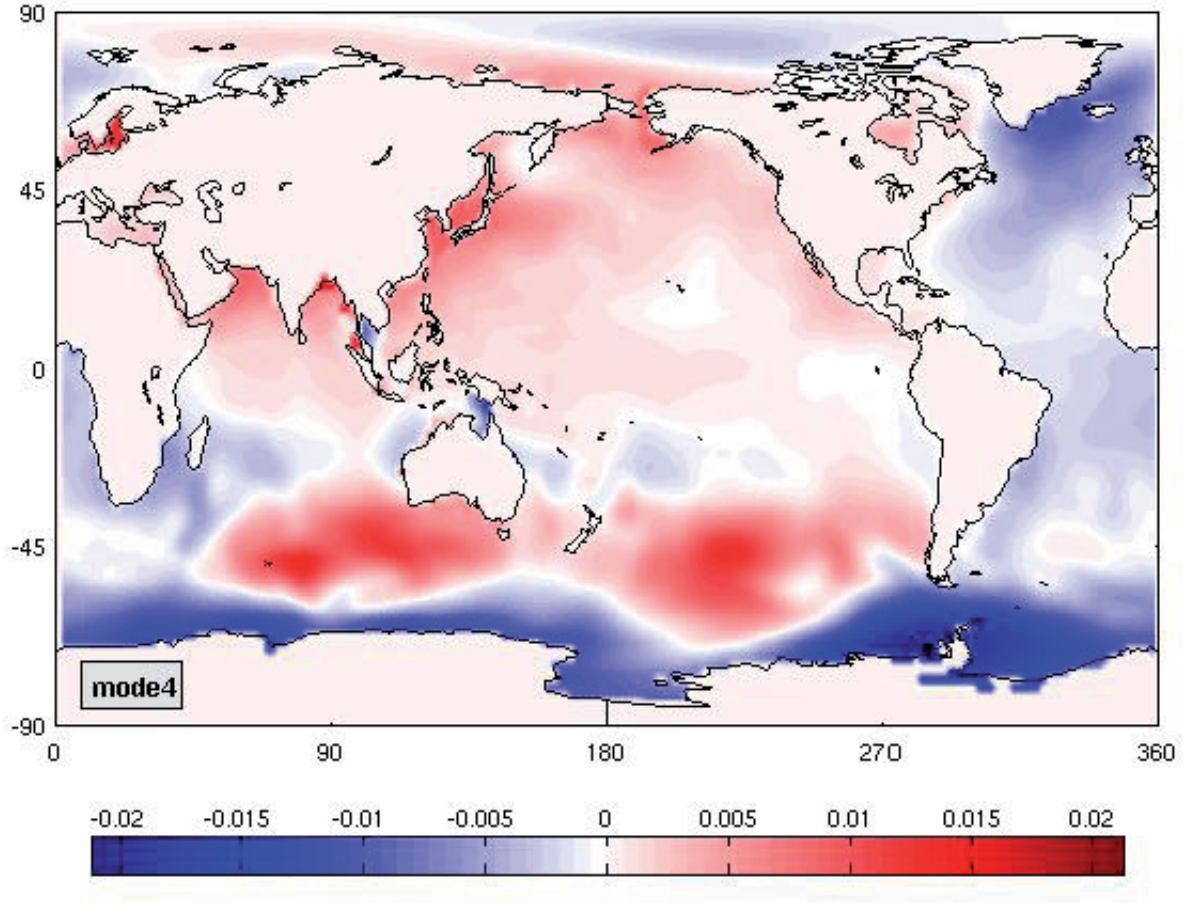

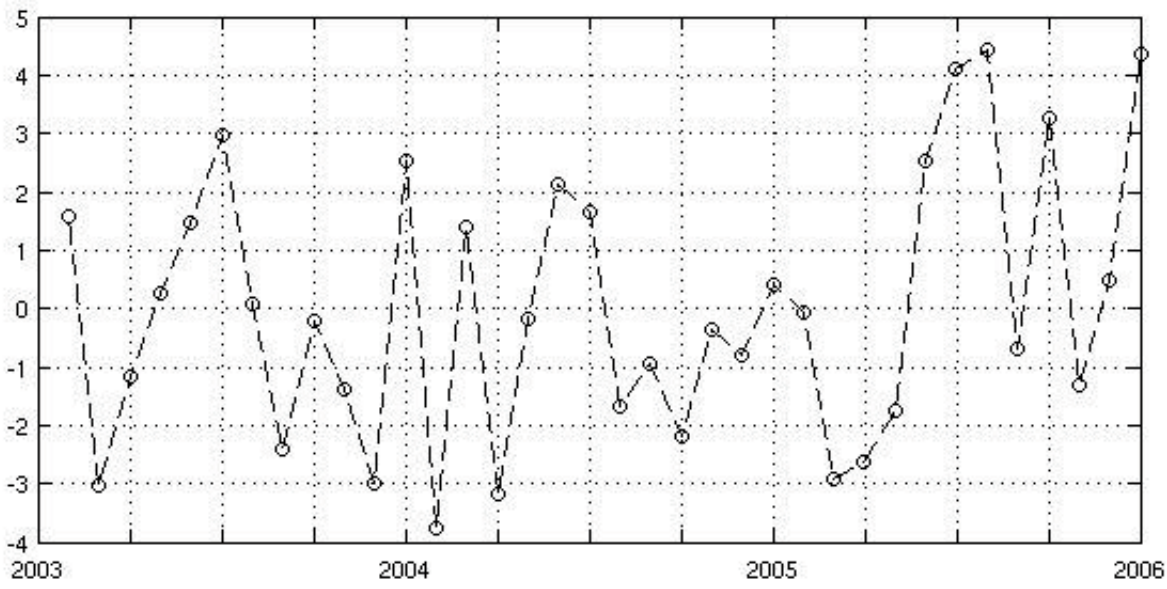

A8: Eigenvector (upper panel) and principal components (lower panel) of mode 4 for the compartment ocean

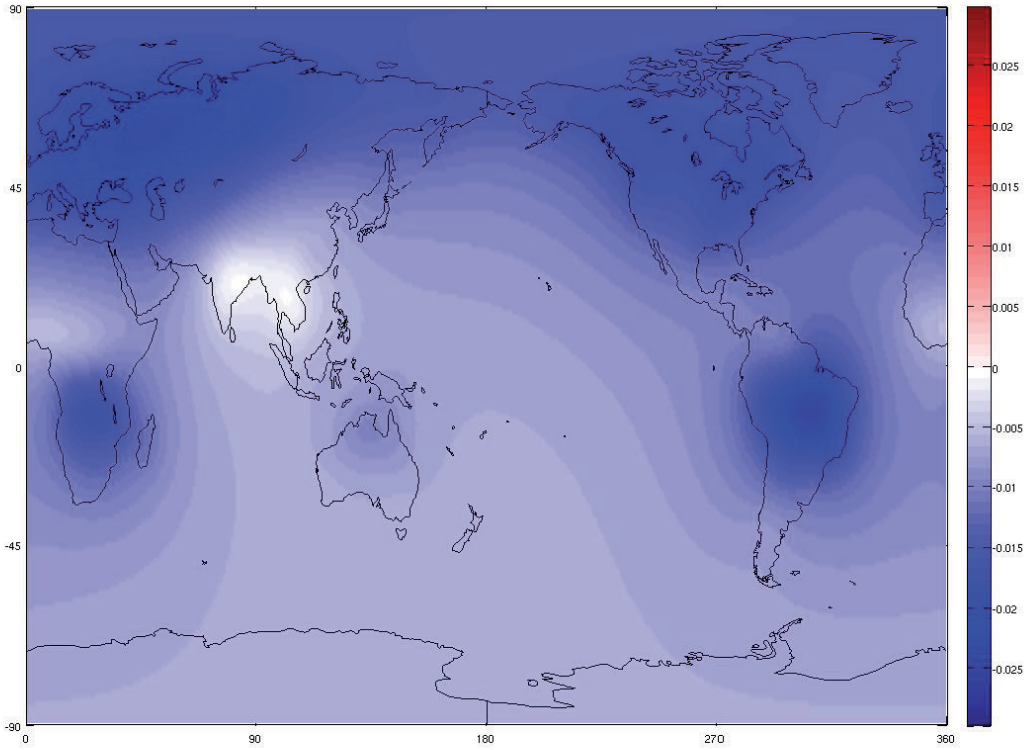

Integro-base-function of mode 1 for the compartment continental hydrolodgy for the GRACE orbit height r =R + 500 km

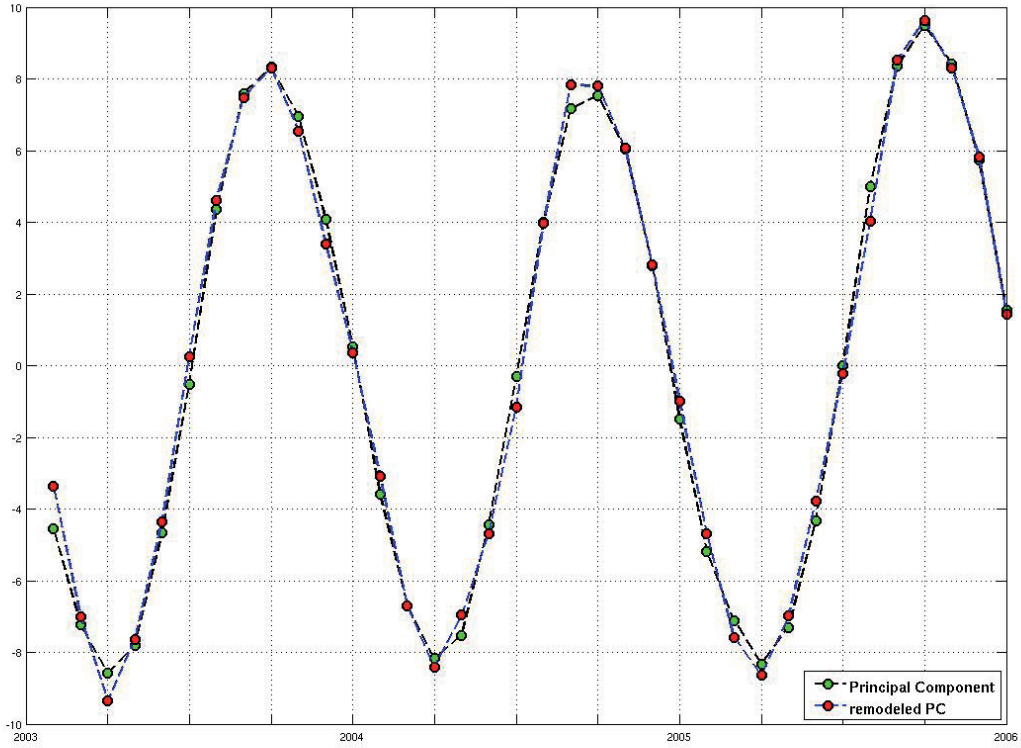

A9: Principal components (original and estimated) for the compartment continental hydrology of mode 1

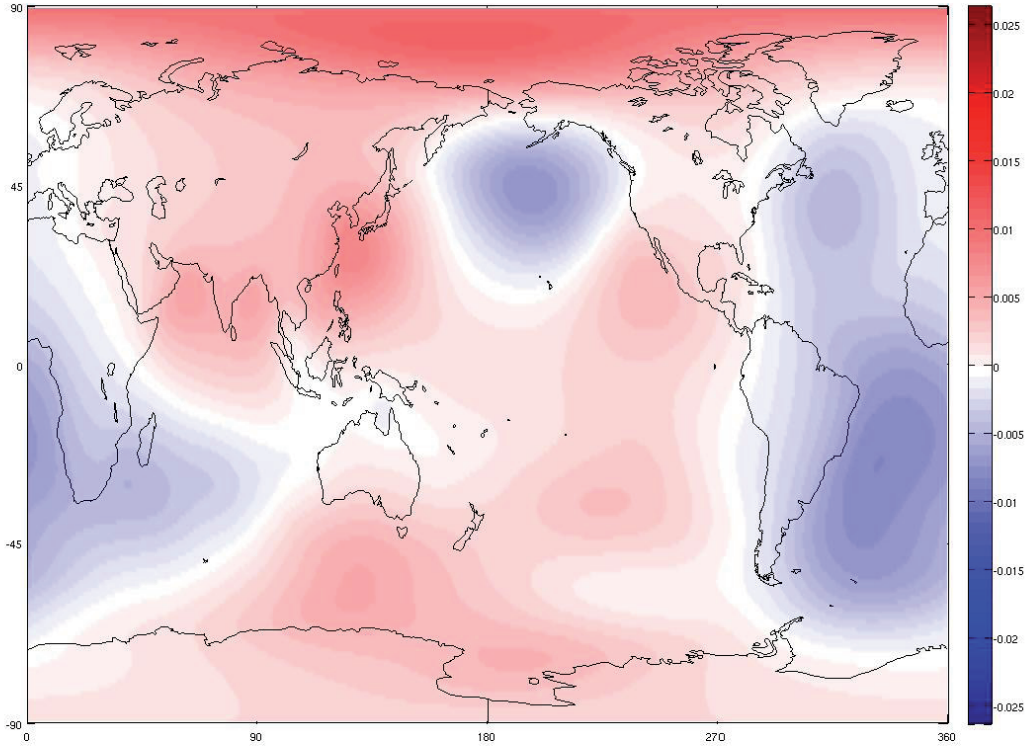

Integro-base-function of mode 1 for the compartment ocean for the GRACE orbit height r =R + 500 km

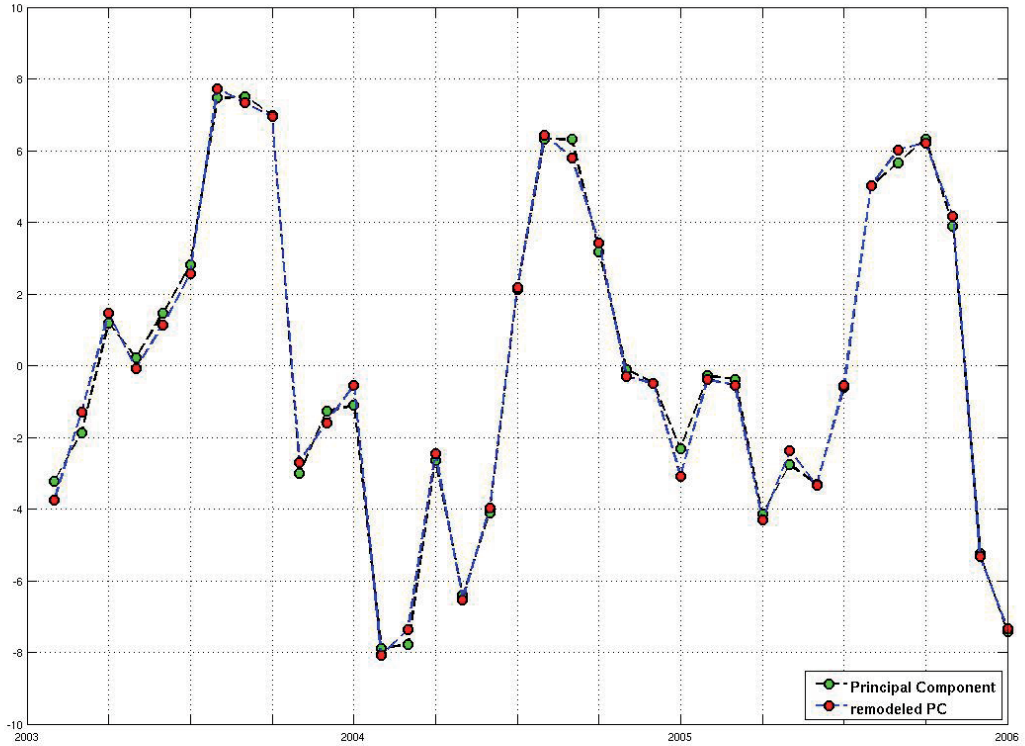

A10: Principal components (original and estimated) for the compartment continental hydrology of mode 1

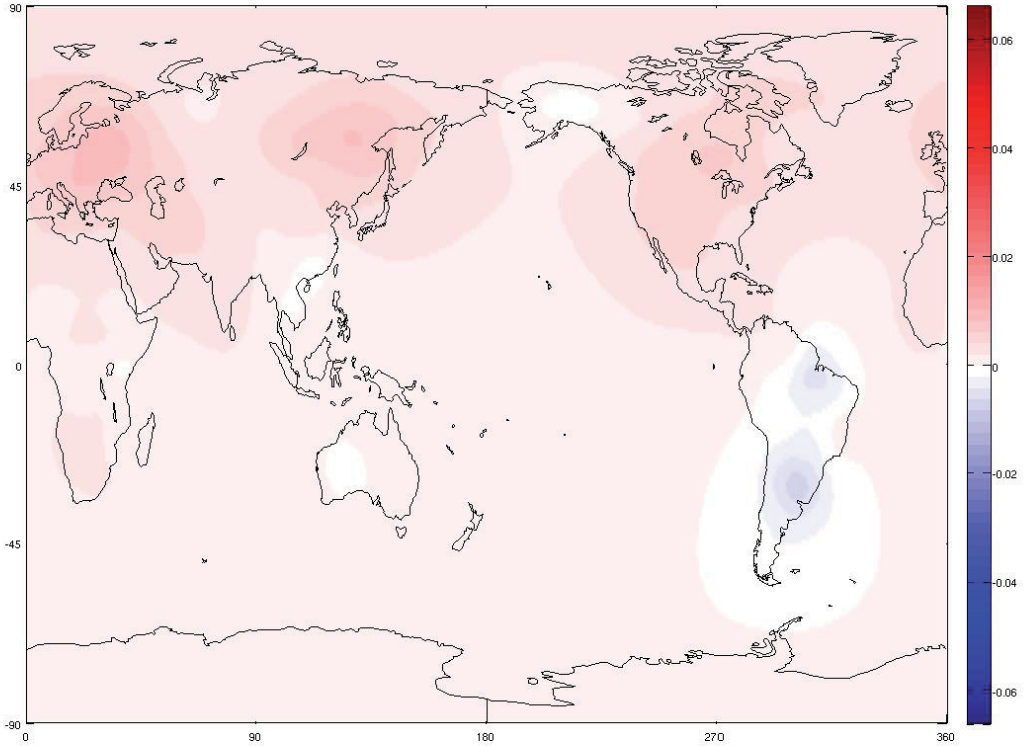

Integro-base-function of mode 2 for the compartment continental hydrology for the GRACE orbit height r =R + 500 km

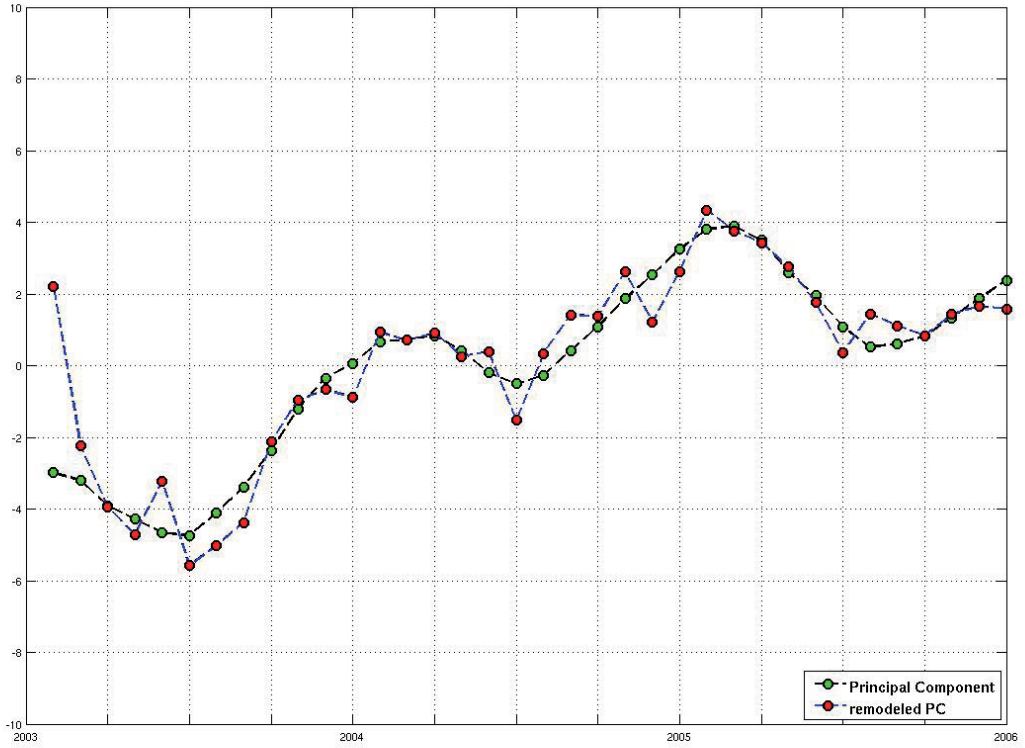

A11: Principal components (original and estimated) for the compartment continental hydrology of mode 2

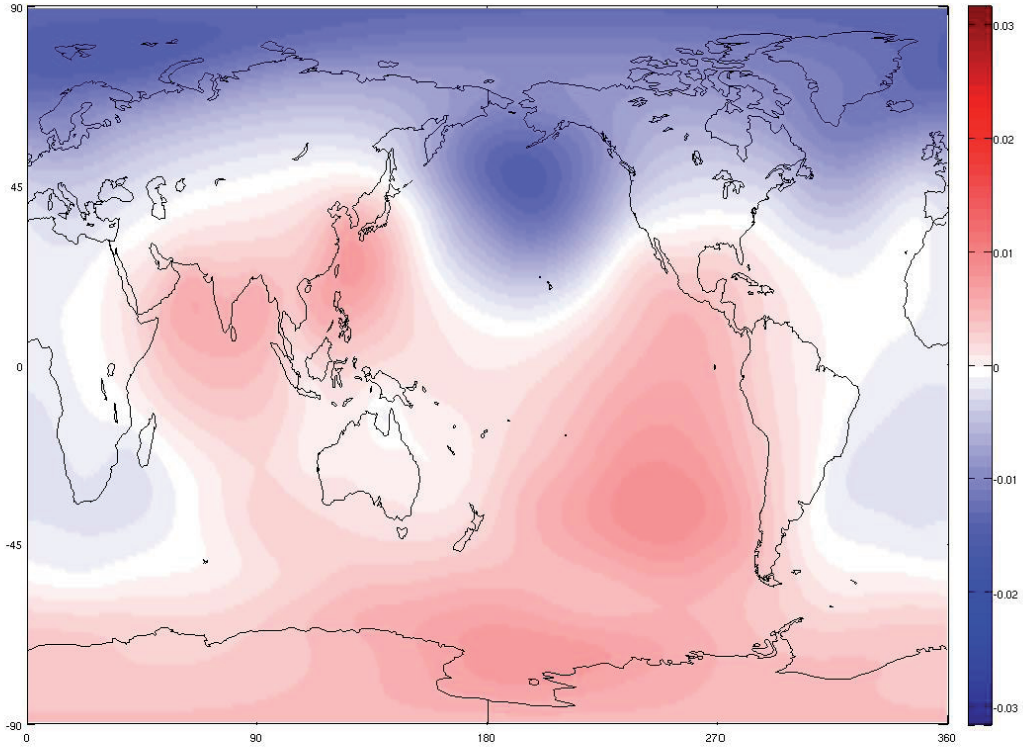

Integro-base-function of mode 2 for the compartment ocean for the GRACE orbit height r =R + 500 km

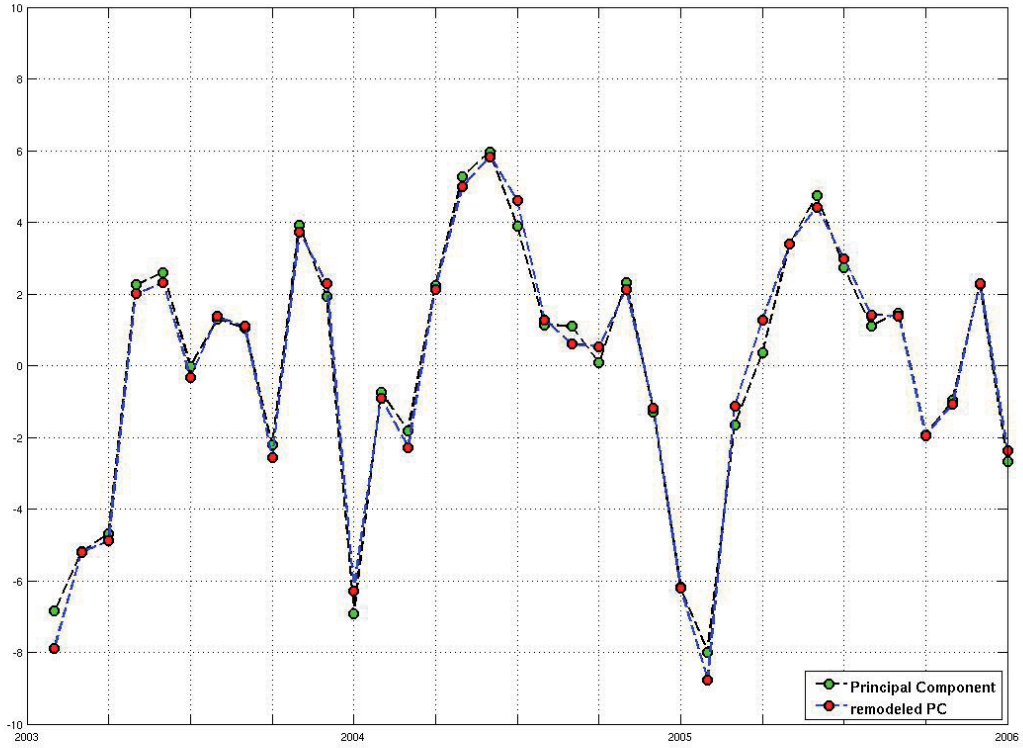

A12: Principal components (original and estimated) for the compartment ocean of mode 2

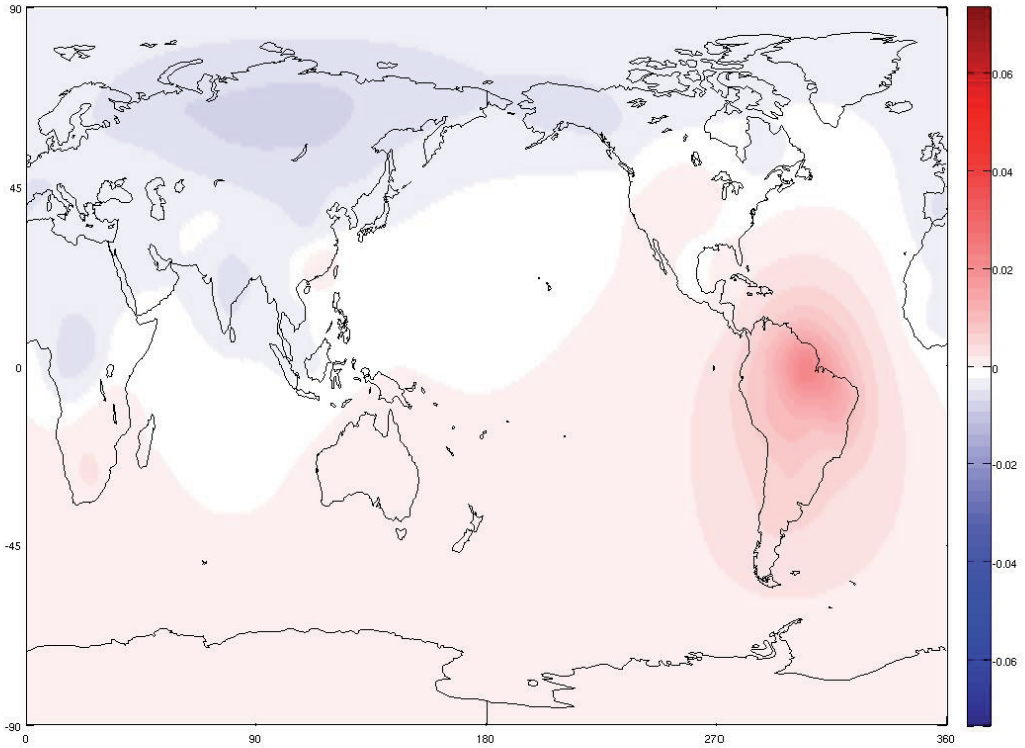

Integro-base-function of mode 3 for the compartment continental hydrology for the GRACE orbit height r =R + 500 km

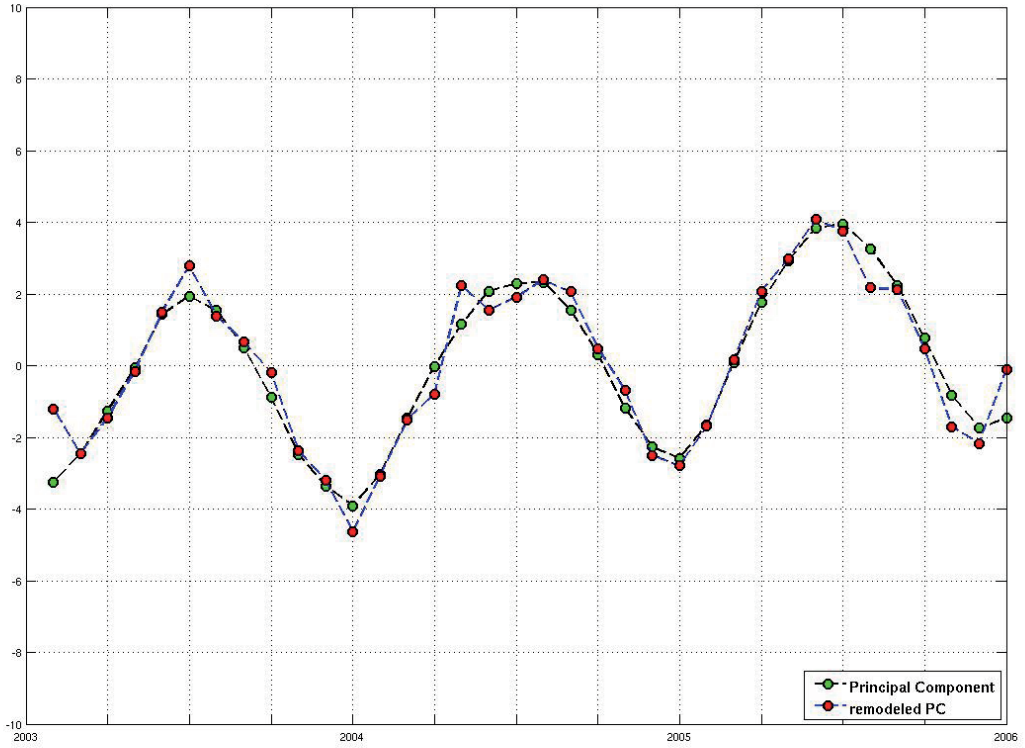

A13: Principal components (original and estimated) for the compartment continental hydrology of mode 3

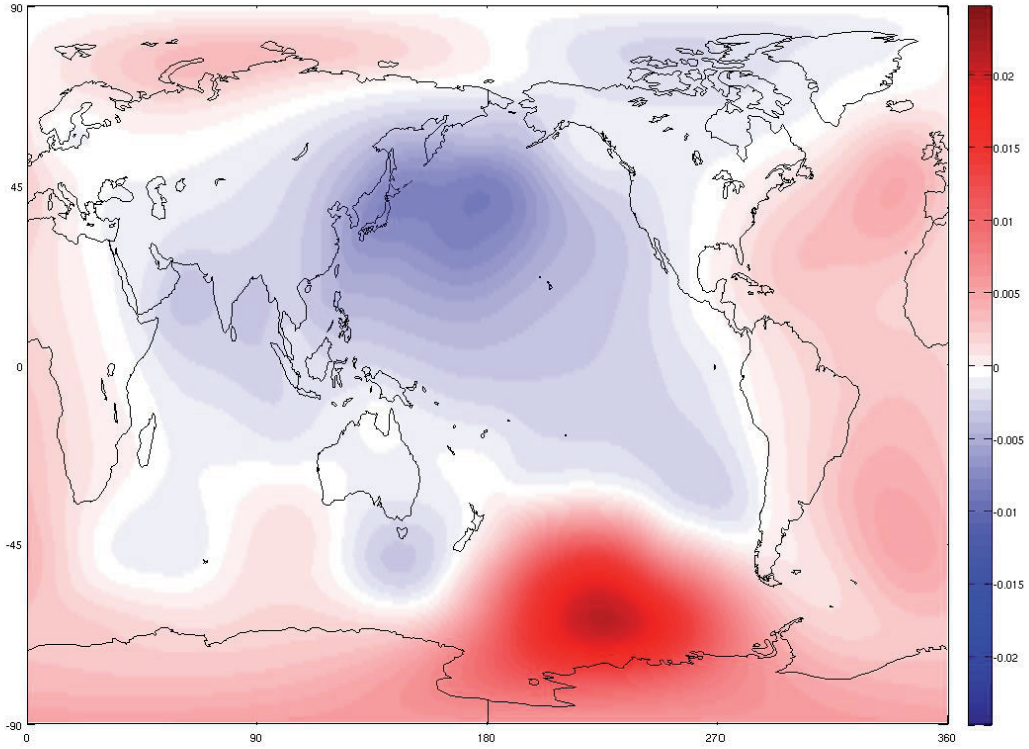

Integro-base-function of mode 3 for the compartment ocean for the GRACE orbit height r =R + 500 km

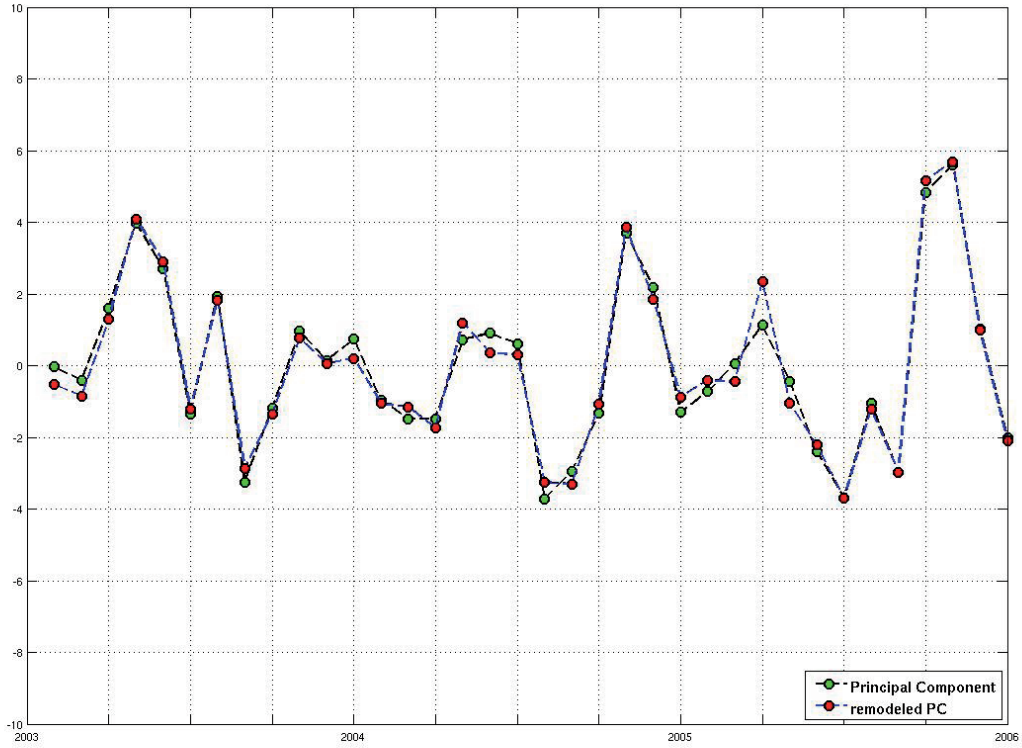

A14: Principal components (original and estimated) for the compartment ocean of mode 3